Main Manuscript for

Epistasis is not a strong constraint on the recurrent evolution of toxin-resistant Na^+,K^+-ATPases among tetrapods.

Shabnam Mohammadi[1,2,*], Lu Yang[3, §,*], Santiago Herrera-Álvarez[4,5,*], María del Pilar Rodríguez-Ordoñez[4,#], Karen Zhang[3], Jay F. Storz[1], Susanne Dobler[2], Andrew J. Crawford[4] & Peter Andolfatto[6]

[1]School of Biological Sciences, University of Nebraska, Lincoln, NE, USA
[2]Molecular Evolutionary Biology, Institute of Zoology, Biocenter Grindel, Universität Hamburg, Hamburg, Germany
[3]Department of Ecology and Evolution, Princeton University, Princeton, NJ, USA
[4]Department of Biological Sciences, Universidad de los Andes, Bogotá, 111711, Colombia
[5]Department of Ecology and Evolution, University of Chicago, Chicago, IL, USA
[6]Department of Biological Sciences, Columbia University, New York, NY, USA

*Co-first authorship

§ Current address: Wellcome Sanger Institute, Cambridge, United Kingdom
# Current address: Université Paris-Saclay Evry, Evry, France

Email: andrew@dna.ac, pa2543@columbia.edu

SM: 0000-0003-3450-6424, LY: 0000-0002-2694-1189, SHA: 0000-0002-0793-7811, MPRO: 0000-0002-0856-1297, KZ: 0000-0003-4406-9977, JFS: 0000-0001-5448-7924, SD: 0000-0002-0635-7719, AJC: 0000-0003-3153-6898, PA: 0000-0003-3393-4574

Classification
Biological Sciences; Evolution

Keywords
Epistasis, protein evolution, cardiotonic steroids, toxin resistance, adaptation

Author Contributions
PA and AJC conceived of and oversaw the project; SM, JFS, SD, AJC and PA designed experiments; KZ, LY, MPRO, SHA, SM collected data; SM, SHA and PA performed evolutionary and statistical analyses; SM, SHA, and PA wrote the paper; All authors edited the manuscript.

This PDF file includes:
Main Text
Figures 1 to 6

Abstract

Comparative genomic studies reveal a global decline in rates of convergent amino acid substitution as a function of evolutionary distance. This pattern has been attributed to epistatic constraints on protein evolution, the idea being that mutations tend to confer the same fitness effects on more similar genetic backgrounds, so convergent substitutions are more likely to occur in closely related species. However, this hypothesis lacks experimental validation. We tested this model in the context of the recurrent evolution of resistance to cardiotonic steroids (CTS) across diverse groups of tetrapods, which occurs via specific amino acid substitutions to the α-subunit family of Na^+,K^+-ATPases (ATP1A). After identifying a series of recurrent substitutions at two key sites of ATP1A1 predicted to confer CTS resistance, we performed protein engineering experiments to test the functional consequences of introducing these substitutions onto divergent species backgrounds. While we find that substitutions at these sites can have substantial background-dependent effects on CTS resistance, we also find no evidence for background-dependent effects on protein activity. We further show that the magnitude of a substitution's effect on activity does not depend on the overall extent of ATP1A1 sequence divergence between species. More generally, a global analysis of substitution patterns across ATP1A orthologs and paralogs reveals that the probability of convergent substitution protein-wide is not predicted by sequence divergence. Together, these findings suggest that intramolecular epistasis is not an important constraint on the evolution of ATP1A CTS resistance in tetrapods.

Significance Statement

Individual amino acid residues within a protein work in concert to produce a functionally coherent structure that must be maintained even as orthologous proteins in different species diverge over time. Given this dependence, we expect identical mutations to have more similar effects on protein function in more closely related species. We tested this hypothesis by performing protein-engineering experiments on ATP1A, an enzyme mediating target-site insensitivity to cardiotonic steroids (CTS) in diverse animals. These experiments reveal that although the phenotypic effects of substitutions can sometimes be background-dependent, the magnitude of these effects does not correlate with ATP1A1 sequence divergence. This implies that the genetic background across the ATP1A protein does not strongly limit the evolution of CTS resistance in animals.

Main Text

Introduction

Patterns of molecular parallelism and convergence represent a useful paradigm to examine the factors that limit the rate of adaptation and the extent to which adaptive evolutionary paths are predictable (1, 2). In the context of protein evolution, patterns of parallelism and convergence are influenced by pleiotropy (the effect of a given mutation on multiple phenotypes) and intramolecular epistasis (nonadditive interactions between mutant sites in the same protein) (3–11). If the phenotypic and fitness effects of mutations depend on the genetic background on which they arise (i.e. epistasis), a given mutation is expected to have more similar effects in orthologs from closely related species. Therefore, the probability of parallel or convergent substitution resulting in sequence divergence between species is expected to decrease with divergence time. Consistent with this expectation, there is evidence for such a decline in broad-scale phylogenetic comparisons of mitochondrial (12) and nuclear (13, 14) proteins. However, this hypothesis has not been tested experimentally to date.

To address the question of how changes in the genetic background alter the phenotypic effects of new mutations, we focus on the test case of the repeated evolution of resistance to cardiotonic steroids (CTS) in animals. CTS are potent inhibitors of Na^+,K^+-ATPase (NKA), a protein that plays a critical role in maintaining membrane potential and is consequently vital for the maintenance of many physiological processes and signaling pathways in animals (15). NKA (Fig. 1A) is a heterodimeric transmembrane protein that consists of a catalytic α-subunit (ATP1A) and a glycoprotein β-subunit (ATP1B) (16). CTS inhibit NKA function by binding to a highly conserved domain of ATP1A and blocking the exchange of Na^+ and K^+ ions (15). NKA is thus often the target of parallel evolution of CTS resistance in insect herbivores that feed on toxic plants (17, 18) as well as vertebrate predators that feed on toxic prey (19–22). Functional investigations of CTS resistance-conferring substitutions in Drosophila (23, 24) and Neotropical grass frogs (25) revealed associated negative pleiotropic effects on protein function and showed that substitutions elsewhere in the protein mitigate these effects. However, despite these examples, the generality of these patterns, and specifically the predicted dependence on evolutionary distance, remain poorly understood given the limited availability of comparative functional data.

Broad phylogenetic comparisons in vertebrates have focused primarily on the H1-H2 extracellular loop of ATP1A proteins, a subset of the CTS-binding domain that contains two sites (111 and 122) known to underlie CTS resistance in rats and toad-eating frogs (25, 26). Most vertebrates possess three paralogs of the α-subunit gene (ATP1A) that have different tissue-specific expression profiles and are associated with distinct physiological roles (Fig. 1B) (15, 27). Mammals possess a fourth

paralog that is expressed predominantly in testes (28). A major limitation of studies to date is that the H1-H2 extracellular loop has been inconsistently surveyed among vertebrate taxa, with previous studies focusing on ATP1A3 in reptiles (20, 21, 29, 30), ATP1A1 and/or ATP1A2 in birds and mammals (30, 31), and either ATP1A1 or ATP1A3 in amphibians (19, 30). We therefore lack a comprehensive survey of amino acid variation in the ATP1A protein family across vertebrates.

To bridge this gap, we first surveyed variation in near full-length coding sequences of the three NKA α-subunit paralogs (ATP1A1, ATP1A2, ATP1A3) that are shared across major extant tetrapod groups (mammals, birds, non-avian reptiles, and amphibians), and identified substitutions that occur repeatedly among divergent lineages. Focusing on two key sites implicated in CTS resistance across animals (111 and 122), we tested whether substitutions at these sites have increasingly distinct phenotypic effects on more divergent genetic backgrounds. Specifically, we engineered several common substitutions at sites 111 and 122 of ATP1A1 that differ between species to reveal potential 'cryptic' epistasis (8, 32). By quantifying the level of CTS resistance conferred by these substitutions, as well as their effects on enzyme function, we evaluate the extent to which pleiotropy and epistasis have constrained the evolution of CTS-resistant forms of ATP1A1 across tetrapods.

Results

Patterns of ATP1A sequence evolution across species and paralogs.

To obtain a more comprehensive portrait of ATP1A amino acid variation among tetrapods, we created multiple sequence alignments for near full-length ATP1A proteins for the three ATP1A paralogs shared among vertebrates. In addition to publicly available data, we generated new RNA-seq data for 27 non-avian reptiles (PRJNA754197) (Table S1-S2). We then *de novo* assembled full-length transcripts of all ATP1A paralogs using these and RNA-seq data from 18 anuran species (25) (PRJNA627222) to achieve better representation for these groups. In total, this dataset comprises 429 species for ATP1A1, 197 species for ATP1A2 and 204 species for ATP1A3 (831 sequences total; Supplemental Dataset 1, Fig. S1).

Our survey reveals numerous substitutions at sites implicated in CTS resistance of NKA (Fig. 2; Supplementary Dataset 2; for comparison to insects, see Supplemental file 1 of ref. (23)). As anticipated from studies of full-length sequences in insects (17, 18, 23), most amino acid variation among species and paralogs is concentrated in the H1-H2 extracellular loop (residues 111-122; Fig 1A). Despite harboring just 28% of 43 sites previously implicated in CTS resistance (33), the

143 H1-H2 extracellular loop contains 81.4% of all substitutions identified among the three ATP1A
144 paralogs (Fig. S2).

145 Our survey reveals several clade- and paralog-specific patterns. Notably, ATP1A1 exhibits more
146 variation among species at sites implicated in CTS resistance (Fig. 2). Most of the variation in
147 ATP1A2 at these sites is restricted to squamate reptiles and ATP1A3 lacks substitutions at site 122
148 altogether, despite the well-known potential for substitutions at this site to confer CTS resistance
149 (25, 26). Looking across species and paralogs, the extent of parallelism at sites 111 and 122 is
150 remarkable (Figs. 2-3): for example, the substitutions Q111E, Q111T, Q111H, Q111L, and Q111V
151 all occur in parallel in multiple species of both insects and vertebrates. N122H and N122D also
152 frequently occur in parallel in both of these major clades. The frequent parallelism of CTS-sensitive
153 (i.e. Q111 and N122) to CTS-resistant states at these sites has been interpreted as evidence for
154 adaptive significance of these substitutions (17–20), but may also reflect mutation biases (34) and
155 the nature of physico-chemico constraints (13, 35).

156 In contrast, some parallelism is restricted to specific clades: for example, Q111R occurs in parallel
157 across tetrapods but has not been observed in insects. Similarly, the combination Q111R+N122D
158 has evolved three times independently in ATP1A1 of tetrapods but is not observed in insects.
159 Conversely, insects have evolved Q111V+N122H independently four times, but this combination
160 has never been observed in tetrapods. These patterns suggest that the fitness effects of some
161 CTS-resistant substitutions depend on genetic background, with the result that CTS-resistance
162 evolved via different mutational pathways in different lineages.

163 Beyond known CTS-resistant substitutions at sites 111 and 122, some taxa have evolved other
164 paths to CTS resistance. For example, the Pacman frog (genus *Ceratophyrs*) is known to prey on
165 CTS-containing toads (36) and its ATP1A1 harbors a known CTS-resistant substitution at site 121
166 (D121N, Supplementary Dataset 2). This substitution is rare among vertebrates but has been
167 previously reported in CTS-adapted milkweed bugs (17, 18). Similarly, the known CTS resistance
168 substitution C104Y is observed among many natricid snakes (Supplementary Dataset 2) and CTS-
169 adapted milkweed weevils (18). Chinchilla (*Chinchilla lanigera*) and yellow-throated sandgrouse
170 (*Pterocles gutturalis*) show distinct single-amino acid insertions in the H1–H2 extracellular loop, a
171 characteristic that has been previously associated with CTS resistance in pyrgomorphid
172 grasshoppers (33, 37). Further, *in lieu* of variation at site 122, ATP1A3 of tetrapods harbors
173 frequent parallel substitutions at site 120 (G120R). Interestingly, this site also shows substantial
174 parallel substitution in the ATP1A1 paralog of birds (where N120K occurs eight times
175 independently) but is mostly invariant in ATP1A1 of other tetrapods.

176

177 **Context-dependent CTS resistance for substitutions at sites 111 and 122**

178

179 The clade- and paralog-specific patterns of substitution among ATP1A paralogs outlined above
180 suggest that the evolution of CTS resistance may be highly dependent on sequence context.
181 However, the functional effects of the vast majority of these substitutions on the diverse genetic
182 backgrounds in which they occur remain largely unknown (25, 26, 29). Given the diversity and
183 broad phylogenetic distribution of parallel substitutions at sites 111 and 122, and the documented
184 effects of some of these substitutions on CTS resistance, we experimentally tested the extent to
185 which functional effects of substitutions at these sites are background-dependent.

186

187 We focused functional experiments on ATP1A1, because it is the most ubiquitously expressed
188 paralog and exhibits both the most sequence diversity and the broadest phylogenetic distribution
189 of parallel substitutions. Specifically, we considered ATP1A1 orthologs from nine representative
190 tetrapod species that possess different combinations of wild-type amino acids at 111 and 122 (Fig.
191 4A). Our taxon sampling includes two lizards, two snakes, two birds, two mammals and previously
192 published data for one amphibian (Fig. S4; Fig. S5; Table S3). The ancestral amino acid states of
193 sites 111 and 122 in tetrapods are Q and N, respectively. We found that the sum of the number of
194 derived states at positions 111 and 122 is a strong predictor of the level of CTS-resistance (Fig 4B,
195 IC_{50}, Spearman's r_S=0.85, p=0.001). Nonetheless, we also found greater than 10-fold variation in
196 CTS-resistance among enzymes that had identical paired states at 111 and 122 (e.g., compare
197 chinchilla (CHI) versus red-necked keelback snakes (KEE) or compare rat (RAT) versus the
198 resistant paralog of grass frogs (GRA_R)). These differences suggest that substitutions at other sites
199 also contribute to CTS resistance.

200

201 To test for epistatic effects of common CTS-resistant substitutions at sites 111 and 122, we used
202 site-directed mutagenesis to introduce 15 substitutions (nine at position 111 and six at position 122)
203 in the wildtype ATP1A1 backgrounds of 9 different species (Fig. S4). The specific substitutions
204 chosen were either phylogenetically broadly-distributed parallel substitutions and/or divergent
205 substitutions that distinguish closely related clades of species. We expressed each of these 24
206 ATP1A1 constructs with an appropriate species-specific ATP1B1 protein (Table S3). For each
207 recombinant NKA protein complex, we characterized its level of CTS resistance (IC_{50}) and we
208 estimated enzyme activity as the rate of ATP hydrolysis in the absence of CTS (Table S4).

209

210 Of the 12 substitutions for which IC_{50} could be measured, substitutions had a 15-fold effect on
211 average (Fig. 4C, Table S4) and were equally likely to increase or decrease IC_{50}. To assess the

background-dependence of specific substitutions, we examined five cases in which a given substitution (e.g., E111H), or the reverse substitution (e.g., H111E), could be evaluated on two or more backgrounds. In the absence of intramolecular epistasis, the effect of a substitution in different backgrounds should remain unchanged and the magnitude of the effect of the reverse substitution should also be the same but with opposite sign. This analysis revealed substantial background dependence for IC_{50} in two of the five informative cases (Fig. 4E; Table S5). In one case, the N122D substitution results in a 200-fold larger increase in IC_{50} when added to the chinchilla (CHI) background compared to the grass frog (GRA) background (p=1.2e-3 by ANOVA). In the other case, the E111H substitution and the reverse substitution (H111E) produced effects in the same direction (reducing CTS-resistance) when added to different backgrounds (false fer-de-lance (FER) and red-necked keelback (KEE) snakes, respectively, p=1e-7 by ANOVA). Overall, these results suggest that the effect of a given substitution on IC_{50} can be strongly dependent on the background on which it occurs. The remaining three substitutions (H111T, Q111R and H122D) showed no significant change in the magnitude of the effect on IC_{50} when introduced into different species' backgrounds. These results suggest that, while some substitutions can have strong background-dependent effects, strong intramolecular epistasis with respect to CTS resistance is not universal.

Pleiotropic effects on NKA activity exhibit little evidence for background-dependence.

We next tested whether substitutions at sites 111 and 122 have pleiotropic effects on ATPase activity. Because ion transport across the membrane is a primary function of NKA and its disruption can have severe pathological effects (38), mutations that compromise this function are likely to be under strong purifying selection. As suggested by previous work (23–25), CTS-resistant substitutions at sites 111 and 122 can decrease enzyme activity. We evaluated the generality of these effects by comparing enzyme activity of the 15 mutant NKA proteins to their corresponding wild-type proteins.

Interestingly, the wild-type enzymes themselves exhibit substantial variation in activity, from 3-18 nmol/mg*min (P = 6e-7 by ANOVA, Fig 4D; Table S4). On average, substitutions at sites 111 and 122 changed enzyme activity by 60% (Fig 4D; Fig S4). In two cases, amino acid substitutions at position 122 (N122H and H122D) nearly inactivate lizard NKAs and, in one case, a substitution at position 111 (Q111T) resulted in low expression of the recombinant protein in the transfected cells (Fig S5; Fig. S6). A test of uniformity of pairwise t-test p-values across substitutions suggests a significant enrichment of low p-values (Fig 4D inset; p=2.5e-4, chi-squared test of uniformity). Thus, globally, this set of substitutions has significant effects on NKA activity, but they were not

247 significantly more likely to decrease than increase activity (10 decrease: 5 increase, p>0.3, binomial
248 test, Fig. 4D, Table S5).
249
250 We next asked to what extent pleiotropic effects of CTS resistant substitutions at positions 111 and
251 122 are dependent on genetic background. This question is motivated by recent studies in insects
252 which revealed that deleterious pleiotropic effects of some resistance-conferring substitutions at
253 sites 111 and 122 are background-dependent (23, 24). Likewise, recent work on ATP1A1 of toad-
254 eating grass frogs showed that effects of Q111R and N122D on NKA activity are background-
255 dependent (25). In contrast, among the five informative cases in which we compared the same
256 substitution (or the reverse substitution) on two or more backgrounds, there is little evidence for
257 background dependence (Fig 4E; Table S5). For example, N122D has similar effects on NKA
258 activity in grass frog and chinchilla despite the substantial divergence between the species' proteins
259 (8.4% protein sequence divergence; Fig. 4D). Similarly, the effects of Q111R in ostrich or the
260 reverse substitution R111Q in sandgrouse were not significantly different from the effect of Q111R
261 in grass frog (7.5% and 8% protein sequence divergence, respectively).
262
263 To further examine the evidence for background dependence, we tested whether changes to the
264 same amino acid state (regardless of starting state) at 111 and 122 produce different changes in
265 NKA activity (e.g., R111E on the rat background versus H111E on the false fer-de-lance
266 background). If epistasis is important, we expect that the difference in effects of substitutions to a
267 given amino acid state should increase with increasing sequence divergence compared to ATP1A1
268 backgrounds in which that state is wild-type. However, across the 11 possible comparisons, we
269 found no relationship between the difference in the effect of substitutions to the same state and the
270 extent of amino acid divergence between the orthologous proteins (Fig. 5). This pattern suggests
271 that, while pleiotropic effects can be background dependent (23, 25), these effects are not
272 pervasive across species and do not correlate with overall sequence divergence.
273
274
275 **The overall rate of convergence across ATP1A proteins does not depend on sequence**
276 **divergence.**
277
278 If intramolecular epistasis is pervasive, we would predict that rates of convergent substitution
279 should decrease as a function of overall sequence divergence (12–14). In contrast to this
280 expectation, our experiments suggest that, for ATP1A1, the extent of background sequence
281 divergence is a poor predictor of the magnitude of effects of substitutions at sites 111 and 122 on
282 CTS resistance and enzyme activity. Since our experiments were necessarily limited in scope, we

carried out a broad phylogenetic analysis to evaluate how well our findings align with global estimates of rates of convergence for the ATP1A family beyond ATP1A1 and beyond sites implicated in CTS resistance.

Using a multisequence alignment of 831 ATP1A protein sequences, including the three ATP1A paralogs shared among tetrapods (i.e., amphibians, non-avian reptiles, birds, and mammals), we inferred a maximum likelihood phylogeny of the gene family (Fig. S1). We then used ancestral sequence reconstruction to infer the history of substitution events on all branches in the tree and counted the number of convergent amino acid substitutions along the protein per site (see Materials and Methods). Convergent substitutions are defined as substitutions on two branches at the same site resulting in the same amino acid state. Interestingly, we do not detect a correlation between the relative number of convergent substitutions with background ATP1A divergence across the tree (Fig. 6A). This result also holds true when considering only substitutions to the key CTS resistance sites 111 and 122 (Fig. S5).

To gain more insight into the factors that determine convergent evolution in ATP1A, we looked more closely at patterns of individual convergent substitutions at sites 111 and 122 by extracting each convergent substitution and visualizing its distribution along the sequence divergence axis (Fig. 6B). Under the expectation that rates of convergence should tend to decrease as a function of sequence divergence, the distribution of pairwise convergent events along the sequence divergence axis should be left-skewed, with a peak towards lower sequence divergence. In contrast to this expectation, the distribution is bimodal, with one peak at 0.33 and the other at 0.69 substitutions/site (Fig. 6B bottom panel). Parallel and convergent substitutions have occurred almost across the full range of protein divergence estimates. For example, if X is any starting state, the substitution X111R has occurred independently in 13 tetrapod lineages and X111L independently in 20 lineages. Both substitutions have a broad phylogenetic distribution, suggesting that their effects do not strongly depend on overall genetic background. Interestingly, however, the distributions for X111H and X111E substitutions are relatively right-skewed, in line with epistasis for CTS resistance that we observed in experiments for H111E/E111H (Fig 4E). Overall, the results of these analyses align well with our functional experiments but run contrary to expectations based on previously reported proteome-wide evolutionary trends (12–14).

Discussion

Previous work has suggested that rates of convergent amino-acid substitution generally decline as a function of time, a pattern that can potentially be explained by epistatic constraints. According to

this view, the higher the level of sequence divergence between a given pair of homologs, the higher the probability that the same mutation will have different fitness effects on the two backgrounds (12). In that respect, our broad survey of the ATP1A gene family in tetrapods, in combination with previous work, reveals two striking and seemingly contradictory patterns. The first is that some substitutions underlying CTS resistance in tetrapods are broadly distributed phylogenetically and even shared with insects (e.g., N122H is widespread among snakes and found in the monarch butterfly and other insects; see Fig. 3 for more examples). Patterns like these suggest that epistatic constraints have a limited role in the evolution of CTS resistance, as the same mutation can be favored on highly divergent genetic backgrounds. On the other hand, there is also substantial diversity in resistance-conferring states at sites 111 and 122, and some combinations of these substitutions appear to be phylogenetically restricted. For example, the CTS-resistant combination of Q111R+N122D has evolved multiple times in tetrapods but is absent in insects, whereas the CTS-resistant combination Q111V+N122H evolved multiple times in insects but is absent in tetrapods (Fig 3). Additionally, some substitutions also appear to be paralog-specific in tetrapods (Fig 3). These phylogenetic signatures suggest at least some role for epistasis as a source of contingency in the evolution of ATP1A-mediated CTS resistance in animals (i.e., the fitness effects of substitutions depend on the order in which they occur). How can these disparate patterns be reconciled? To what extent do genetic background and contingency limit the evolution of CTS resistance in animals?

In our survey of putative CTS-resistant substitutions at sites 111 and 122, we find that derived substitutions have largely predictable effects on CTS resistance, with notable exceptions that tend to be in magnitude rather than direction (Fig. 4C and 4E). While derived states at sites 111 and 122 are generally a reliable predictor of CTS resistance (Fig. 4A), they do not always predict the effect size of particular substitutions (e.g., Q111R contributes to CTS resistance on many species' backgrounds, but not on that of sandgrouse, Fig. 4C). It is also notable that species with identical paired states at 111 and 122 can vary in CTS resistance by more than an order of magnitude. Both patterns point to background determinants of CTS resistance that may be additive rather than epistatic. Yet there are some broadly phylogenetically distributed substitutions, such as N122D, that nonetheless do exhibit background-dependent effects on CTS resistance (Fig. 4C and 4E).

While epistasis is likely to be a pervasive feature in protein evolution, many mutational effects on structural and functional properties of proteins appear to be purely additive (e.g., (39–41). In line with this, our experimental results revealed that the phenotypic effects of individual substitutions on ATPase activity are likely to be additive in general. We also found no correlation between the marginal effect of a substitution with background genetic divergence. Specifically, mutating to the

same amino acid state (irrespective of the initial state) doesn't result in larger effects in more distant backgrounds. Under additivity, the rate of convergence is expected to be uncorrelated with background genetic distance because the phenotypic effect of a mutation does not depend on the amino acid states at other sites in the protein. Our phylogenetic and experimental results align with this expectation.

While the extent to which changes in CTS resistance are favorable to an organism depend on physiological constraints and the specific ecological context (e.g., in which tissues NKA is expressed and the presence of dietary CTS), changes in enzyme activity associated with these substitutions are most likely detrimental to organismal fitness. It follows that changes to the ATP1A1 background would be required to offset such changes in enzyme activity. Surprisingly, we found that, with rare exceptions, CTS-resistant substitutions at sites 111 and 122 tend to exhibit little or no pleiotropy with respect to enzyme activity. In addition, amino acid substitutions were not significantly more likely to decrease rather than increase activity. Interestingly, the activity of wildtype ATP1A1 enzymes varies 6-fold among the species surveyed (Fig. 4E), suggesting that most species are either robust to changes in NKA activity, or that changes have occurred in other genes (including other ATP1A paralogs) that compensate for changes in activity. Thus, it may be that protein activity itself is either not an important pleiotropic constraint on the evolution of ATP1A CTS resistance or that constraint depends not just on the protein background, but also on the background at higher levels (e.g., other interacting proteins). A further possibility is that detrimental effects of CTS resistant substitutions depend on few sites, and these sites are also highly convergent (e.g., A119S among insect herbivores, see refs. 23 and 24).

We conclude that intramolecular epistasis in ATP1A -- at the level of protein activity -- is unlikely to represent a substantial constraint in the evolution of CTS resistance. However, the lack of evidence of epistasis at the level of protein function does not preclude an important role for epistasis at higher levels. For example, our results are also consistent with a scenario of nonspecific (or global) epistasis, where mutations have additive effects on molecular phenotypes (e.g., ATPase activity) but have nonadditive effects on fitness due to a nonlinear relationship between phenotype and fitness (7, 40, 42). Nonspecific epistasis predicts a many-to-one relationship with respect to genetic backgrounds and specific mutations (7, 42), such that many genetic backgrounds can compensate for the deleterious effects of a given mutation. Thus, nonspecific epistasis of this form could explain why CTS resistant substitutions at sites 111 and 122 exhibit broad phylogenetic distributions.

Dependence on few sites, or the many-to-one nature of non-specific epistasis, may also account for the weak signature of decreasing convergence with increasing divergence for ATP1A. Our study

391 suggests that, while intramolecular epistasis may be pervasive across proteomes, it does not
392 always represent a substantial constraint on the evolution of adaptive traits, as we show here for
393 CTS resistance in tetrapods. Further evaluation of epistasis at higher levels than enzyme activity
394 (e.g., whole organism neural function, CTS tolerance or viability, refs. 23, 24) may elucidate the
395 extent to which nonspecific epistasis constrains protein evolution in these cases.
396

Materials and Methods

Sample collection and data sources.

In order to carry out a comprehensive survey of vertebrate ATP1A paralogs, we collated a total of 831 protein sequences for this study (Supplementary Dataset 1). In addition to publicly available data, we also generated RNA-seq data for 27 species of non-avian reptiles (Table S1; PRJNA754197) to achieve a better representation of some previously underrepresented lineages. These included field-caught and museum-archived specimens as well as animals purchased from commercial pet vendors. Purchased animals were processed following the procedures specified in the IACUC Protocol No. 2057-16 (Princeton University) and implemented by a research veterinarian at Princeton University. Wild-caught animals were collected under Colombian umbrella permit *resolución No*. 1177 granted by the *Autoridad Nacional de Licencias Ambientales* to the Universidad de los Andes and handled according to protocols approved by the Institutional Committee on the Care and Use of Laboratory Animals (abbreviated CICUAL in Spanish) of the Universidad de los Andes. In all cases, fresh tissues (brain, stomach, and muscle) were taken and preserved in RNAlater (Invitrogen) and stored at -80ºC until used.

Reconstruction of ATP1A paralogs.

RNA-seq libraries were prepared either using TruSeq RNA Library Prep Kit v2 (Illumina) and sequenced on Illumina HiSeq2500 (Genomics Core Facility, Princeton, NJ, USA) or using NEBNext Ultra RNA Library Preparation Lit (NEB) and sequenced on Illumina HiSeq4000 (Genewiz, South Plainfield, NJ, USA) (Table S2). All raw RNA-seq data generated for this study have been deposited in the National Center for Biotechnology Information (NCBI) Sequence Read Archive (SRA) under bioproject PRJNA754197. Together with SRA datasets downloaded from public database, reads were trimmed to Phred quality ≥ 20 and length ≥ 20 and then assembled *de novo* using Trinity v2.2.0 (43). Sequences of ATP1A paralogs 1, 2 and 3 were pulled out with BLAST searches (blast-v2.26), individually curated, and then aligned using ClustalW. Complete alignments of ATP1/2/3 can be found in Supplementary Dataset 1.

Character state mapping and parameter estimation for the ATP1A1-3 paralogs

Protein sequences from ATP1A1 (N=429), ATP1A2 (N=197) and ATP1A3 (N=205) including main tetrapod groups (amphibians, non-avian reptiles, birds, and mammals) and lungfish+coelacanth as outgroups were aligned using ClustalW with default parameters. The optimal parameters for phylogenetic reconstruction were taken from the best-fit amino acid substitution model based on Akaike Information Criterion (AIC) as implemented in ModelTest-NG v.0.1.5 (44), and was inferred to be JTT+G4+F. An initial phylogeny was inferred using RAxML HPC v.8 (45) under the JTT+GAMMA model with empirical amino acid frequencies. Branch lengths and node support

(aLRS) were further refined using PhyML v.3.1 (46) with empirical amino acid frequencies and maximum likelihood estimates of rate heterogeneity parameters, I and Γ. Phylogeny visualization and mapping of character states for each paralog was done using the R package ggtree (47).

Ancestral sequence reconstruction and convergence calculations

Ancestral sequence reconstruction (ASR) was performed in PAML using codeml (48) under the JTT+G4+F substitution model. Statistical confidence in each position's reconstructed state for each ancestor was determined from the posterior probability (PP), and only states with PP>0.8 were considered. Ancestral sequences from all nodes in the ATP1A phylogeny were retrieved from the codeml output, resulting in an alignment of 1,660 ATP1A proteins (831 extant species and 829 inferred ancestral sequences; Fig. S1). For each branch in the tree, we determined the occurrence of substitutions by using the ancestral and derived amino acid states at each site using only states with PP>0.8. All branch pairs were compared, except sister branches and ancestor-descendent pairs (12, 13). When comparing substitutions on two distinct branches at the same site, substitutions to the same amino acid state were counted as convergences, while substitutions away from a common amino acid were counted as divergences. An alignment of 1,040 amino acids was used to calculate the number of molecular convergences and divergences, excluding a putative 30 amino acid-long alternative spliced region (positions 834-864). Model-based estimates of sequence divergence, number of convergences, number of divergences, and total number of substitutions since the common ancestor were recorded for each pairwise comparison. We calculated the proportion of observed convergent events per branch as (number of convergences +1) / (number of divergences +1). The line describing the trend was calculated as a running average with window size of 0.05 substitutions/site. 95% confidence intervals were calculated based on 100 bootstrap replicates per window, resampling only variable sites.

For sites 111 and 122, molecular convergence was coded as "1" when the substitution along $branch_i$ was to the same amino acid state as the substitution along $branch_j$, and "0" if substitutions were to different states. Model-based estimates of sequence divergence, amino acid state, and convergence event were recorded for each pairwise comparison (when convergence was "0", amino acid state was set to "NA"). A logistic regression between molecular convergence (0 or 1) and genetic distance was used to test for the correlation between variables (Fig 6B; Fig. S3)

Construction of expression vectors.

ATP1A1 and ATP1B1 wild-type sequences for the eight selected tetrapod species (Fig 4) were synthesized by Invitrogen^{TM} GeneArt. The β1-subunit genes were inserted into pFastBac Dual expression vectors (Life Technologies) at the p10 promoter with XhoI and PaeI (FastDigest Thermo

Scientific™) and then control sequenced. The α1-subunit genes were inserted at the PH promoter of vectors already containing the corresponding β1-subunit proteins using In-Fusion® HD Cloning Kit (Takara Bio, USA Inc.) and control sequenced. All resulting vectors had the α1-subunit gene under the control of the PH promoter and a β1-subunit gene under the p10 promoter. The resulting eight vectors were then subjected to site-directed mutagenesis (QuickChange II XL Kit; Agilent Technologies, La Jolla, CA, USA) to introduce the codons of interest. In total, 21 vectors were produced (Table S3).

Generation of recombinant viruses and transfection into Sf9 cells.

Escherichia coli DH10bac cells harboring the baculovirus genome (bacmid) and a transposition helper vector (Life Technologies) were transformed according to the manufacturer's protocol with expression vectors containing the different gene constructs. Recombinant bacmids were selected through PCR screening, grown, and isolated. Subsequently, Sf9 cells (4 x 10^5 cells*ml) in 2 ml of Insect-Xpress medium (Lonza, Walkersville, MD, USA) were transfected with recombinant bacmids using Cellfectin reagent (Life Technologies). After a three-day incubation period, recombinant baculoviruses were isolated (P1) and used to infect fresh Sf9 cells (1.2 x 10^6 cells*ml) in 10 ml of Insect-Xpress medium (Lonza, Walkersville, MD, USA) with 15 mg/ml gentamycin (Roth, Karlsruhe, Germany) at a multiplicity of infection of 0.1. Five days after infection, the amplified viruses were harvested (P2 stock).

Preparation of Sf9 membranes.

For production of recombinant NKA, Sf9 cells were infected with the P2 viral stock at a multiplicity of infection of 10^3. The cells (1.6 x 10^6 cells*ml) were grown in 50 ml of Insect-Xpress medium (Lonza, Walkersville, MD, USA) with 15 mg/ml gentamycin (Roth, Karlsruhe, Germany) at 27°C in 500 ml flasks (35). After 3 days, Sf9 cells were harvested by centrifugation at 20,000 x g for 10 min. The cells were stored at -80 °C and then resuspended at 0 °C in 15 ml of homogenization buffer (0.25 M sucrose, 2 mM EDTA, and 25 mM HEPES/Tris; pH 7.0). The resuspended cells were sonicated at 60 W (Bandelin Electronic Company, Berlin, Germany) for three 45 s intervals at 0 °C. The cell suspension was then subjected to centrifugation for 30 min at 10,000 x g (J2-21 centrifuge, Beckmann-Coulter, Krefeld, Germany). The supernatant was collected and further centrifuged for 60 m at 100,000 x g at 4 °C (Ultra- Centrifuge L-80, Beckmann-Coulter) to pellet the cell membranes. The pelleted membranes were washed once and resuspended in ROTIPURAN® p.a., ACS water (Roth) and stored at -20 °C. Protein concentrations were determined by Bradford assays using bovine serum albumin as a standard. Three biological replicates were produced for each NKA construct.

Verification by SDS-PAGE/western blotting.

For each biological replicate, 10 μg of protein were solubilized in 4x SDS-polyacrylamide gel electrophoresis sample buffer and separated on SDS gels containing 10% acrylamide. Subsequently, they were blotted on nitrocellulose membrane (HP42.1, Roth). To block non-specific binding sites after blotting, the membrane was incubated with 5% dried milk in TBS-Tween 20 for 1 h. After blocking, the membranes were incubated overnight at 4 °C with the primary monoclonal antibody α5 (Developmental Studies Hybridoma Bank, University of Iowa, Iowa City, IA, USA). Since only membrane proteins were isolated from transfected cells, detection of the α subunit also indicates the presence of the β subunit. The primary antibody was detected using a goat-anti-mouse secondary antibody conjugated with horseradish peroxidase (Dianova, Hamburg, Germany). The staining of the precipitated polypeptide-antibody complexes was performed by addition of 60 mg 4-chloro-1 naphtol (Sigma-Aldrich, Taufkirchen, Germany) in 20 ml ice-cold methanol to 100 ml phosphate buffered saline (PBS) containing 60 μl 30% H_2O_2. See Fig. S6.

Ouabain inhibition assay.

To determine the sensitivity of each NKA construct against cardiotonic steroids (CTS), we used the water-soluble cardiac glycoside, ouabain (Acrōs Organics), as our representative CTS. 100 ug of each protein was pipetted into each well in a nine-well row on a 96-well microplate (Fisherbrand) containing stabilizing buffers (see buffer formulas in (49)). Each well in the nine-well row was exposed to exponentially decreasing concentrations (10^{-3} M, 10^{-4} M, 10^{-5} M, 10^{-6} M, 10^{-7} M, 10^{-8} M, dissolved in distilled H_2O) of ouabain, distilled water only (experimental control), and a combination of an inhibition buffer lacking KCl and 10^{-2} M ouabain to measure background protein activity (49). The proteins were incubated at 37°C and 200 rpms for 10 minutes on a microplate shaker (Quantifoil Instruments, Jena, Germany). Next, ATP (Sigma Aldrich) was added to each well and the proteins were incubated again at 37°C and 200 rpms for 20 minutes. The activity of NKA following ouabain exposure was determined by quantification of inorganic phosphate (Pi) released from enzymatically hydrolyzed ATP. Reaction Pi levels were measured according to the procedure described in Taussky and Shorr (50) (see Petschenka et al. (49)). All assays were run in duplicate and the average of the two technical replicates was used for subsequent statistical analyses. Absorbance for each well was measured at 650 nm with a plate absorbance reader (BioRad Model 680 spectrophotometer and software package). See Table S4.

ATP hydrolysis assay.

To determine the functional efficiency of different NKA constructs, we calculated the amount of Pi hydrolyzed from ATP per mg of protein per minute. The measurements were obtained from the same assay as described above. In brief, absorbance from the experimental control reactions, in

which 100 μg of protein was incubated without any inhibiting factors (i.e., ouabain or buffer excluding KCl), were measured and translated to mM Pi from a standard curve that was run in parallel (1.2 mM Pi, 1 mM Pi, 0.8 mM Pi, 0.6 mM Pi, 0.4 mM Pi, 0.2 mM Pi, 0 mM Pi). See Table S4.

Statistical analyses of functional data.

Background phosphate absorbance levels from reactions with inhibiting factors were used to calibrate phosphate absorbance in wells measuring ouabain inhibition and in the control wells measuring non-inhibited NKA activity (49). For ouabain sensitivity measurements, calibrated absorbance values were converted to percentage non-inhibited NKA activity based on measurements from the control wells (49). These data were plotted and log IC_{50} values were obtained for each biological replicate from nonlinear fitting using a four-parameter logistic curve, with the top asymptote set to 100 and the bottom asymptote set to zero. Curve fitting was performed with the nlsLM function of the minipack.lm library in R. For comparisons of recombinant protein activity, the calculated Pi concentrations of 100 μg of protein assayed in the absence of ouabain were converted to nmol Pi/mg protein/min. IC_{50} values were log-transformed. We used pairwise *t*-tests with Bonferroni corrections to identify significant differences between constructs with and without engineered substitutions. We used a two-way ANOVA to test for background dependence of substitutions (i.e., interaction between background and amino acid substitution) with respect to ouabain resistance (log IC_{50}) and protein activity. Specifically, we tested whether the effects of a substitution X->Y are equal on different backgrounds (null hypothesis: X->Y (background 1) = X->Y (background 2)). We further assumed that the effects of a substitution X->Y should exactly match that of Y->X. All statistical analyses were implemented in R. Data were plotted using the ggplot2 package in R.

Acknowledgments

We thank C. Natarajan, P. Kowalski, M. Winter, and V. Wagschal for assistance in the laboratory, and D.A. Gómez-Sánchez for assistance in the field. We thank J. Oaks for providing tissue from ring-necked snake. **Funding:** This study was funded by grants from the National Institutes of Health to PA (R01-GM115523), JFS (R01-HL087216) and SM (F32–HL149172), the National Science Foundation (OIA-1736249) to JFS, the Deutsche Forschungsgemeinschaft (Do 517/10-1) to SD, and the Alexander von Humboldt Foundation to SM.

References

1. D. L. Stern, The genetic causes of convergent evolution. *Nat. Rev. Genet.* **14**, 751–764 (2013).

2. J. F. Storz, Causes of molecular convergence and parallelism in protein evolution. *Nat. Rev. Genet.* **17**, 239 (2016).

3. D. L. Stern, *Evolution, development, & the predictable genome* (Roberts and Co. Publishers, 2011).

4. P. C. Phillips, Epistasis—the essential role of gene interactions in the structure and evolution of genetic systems. *Nat. Rev. Genet.* **9**, 855–867 (2008).

5. W. Fitch, Rate of change of concomitantly variable codons. *J. Mol. Evol.* **1**, 84–96 (1971).

6. B. Callahan, R. A. Neher, D. Bachtrog, P. Andolfatto, B. I. Shraiman, Correlated evolution of nearby residues in Drosophilid proteins. *PLoS Genet.* **7**, e1001315 (2011).

7. T. N. Starr, J. W. Thornton, Epistasis in protein evolution. *Protein Sci.* **25**, 1204–1218 (2016).

8. J. F. Storz, Compensatory mutations and epistasis for protein function. *Curr. Opin. Struct. Biol.* **50**, 18–25 (2018).

9. D. D. Pollock, G. Thiltgen, R. A. Goldstein, Amino acid coevolution induces an evolutionary Stokes shift. *Proc. Natl. Acad. Sci.* **109**, E1352 (2012).

10. P. Shah, D. M. McCandlish, J. B. Plotkin, Contingency and entrenchment in protein evolution under purifying selection. *Proc. Natl. Acad. Sci.* **112**, E3226 (2015).

11. V. O. Pokusaeva, *et al.*, An experimental assay of the interactions of amino acids from orthologous sequences shaping a complex fitness landscape. *PLoS Genet.* **15**, e1008079 (2019).

12. R. A. Goldstein, S. T. Pollard, S. D. Shah, D. D. Pollock, Nonadaptive amino acid convergence rates decrease over time. *Mol. Biol. Evol.* **32**, 1373–1381 (2015).

13. Z. Zou, J. Zhang, Are convergent and parallel amino acid substitutions in protein evolution more prevalent than neutral expectations? *Mol. Biol. Evol.* **32**, 2085–2096 (2015).

14. Z. Zou, J. Zhang, Gene tree discordance does not explain away the temporal decline of convergence in mammalian protein sequence evolution. *Mol. Biol. Evol.* **34**, 1682–1688 (2017).

15. J. B. Lingrel, The physiological significance of the cardiotonic steroid/ouabain-binding site of the Na, K-ATPase. *Annu. Rev. Physiol.* **72**, 395–412 (2010).

16. A. Koksoy, Na+, K+-ATPase: a review. *J Ank. Med Sch* **24**, 73–82 (2002).

17. S. Dobler, S. Dalla, V. Wagschal, A. A. Agrawal, Community-wide convergent evolution in insect adaptation to toxic cardenolides by substitutions in the Na, K-ATPase. *Proc. Natl. Acad. Sci.* **109**, 13040–13045 (2012).

18. Y. Zhen, M. L. Aardema, E. M. Medina, M. Schumer, P. Andolfatto, Parallel molecular evolution in an herbivore community. *Science* **337**, 1634–1637 (2012).

19. D. J. Moore, D. C. Halliday, D. M. Rowell, A. J. Robinson, J. S. Keogh, Positive Darwinian selection results in resistance to cardioactive toxins in true toads (Anura: Bufonidae). *Biol. Lett.* **5**, 513–516 (2009).

20. B. Ujvari, *et al.*, Widespread convergence in toxin resistance by predictable molecular evolution. *Proc. Natl. Acad. Sci.* **112**, 11911–11916 (2015).

21. S. Mohammadi, *et al.*, Toxin-resistant isoforms of Na+/K+-ATPase in snakes do not closely track dietary specialization on toads. *Proc. R. Soc. B Biol. Sci.* **283**, 20162111 (2016).

22. S. Mohammadi, L. Yang, M. Bulbert, H. M. Rowland, The evolutionary and behavioural ecology of cardiotonic steroid resistance in predators (In prep).

23. A. M. Taverner, *et al.*, Adaptive substitutions underlying cardiac glycoside insensitivity in insects exhibit epistasis in vivo. *eLife* **8**, e48224 (2019).

24. M. Karageorgi, *et al.*, Genome editing retraces the evolution of toxin resistance in the monarch butterfly. *Nature* **574**, 409–412 (2019).

25. S. Mohammadi, *et al.*, Concerted evolution reveals co-adapted amino acid substitutions in frogs that prey on toxic toads. *Curr. Biol.* **31**, 2530-2538.e10 (2021).

26. E. M. Price, J. B. Lingrel, Structure-function relationships in the sodium-potassium ATPase. alpha. subunit: site-directed mutagenesis of glutamine-111 to arginine and asparagine-122 to aspartic acid generates a ouabain-resistant enzyme. *Biochemistry* **27**, 8400–8408 (1988).

27. K. J. Sweadner, *et al.*, Genotype-structure-phenotype relationships diverge in paralogs ATP1A1, ATP1A2, and ATP1A3. *Neurol. Genet.* **5**, e303–e303 (2019).

28. A. Mobasheri, *et al.*, Na+, K+-ATPase isozyme diversity; comparative biochemistry and physiological implications of novel functional interactions. *Biosci. Rep.* **20**, 51–91 (2000).

29. B. Ujvari, *et al.*, Isolation breeds naivety: island living robs Australian varanid lizards of toad-toxin immunity via four-base-pair mutation. *Evol. Int. J. Org. Evol.* **67**, 289–294 (2013).

30. B. M. Marshall, *et al.*, Widespread vulnerability of Malagasy predators to the toxins of an introduced toad. *Curr. Biol.* **28**, R654–R655 (2018).

31. S. Groen, N. Whiteman, Convergent evolution of cardiac-glycoside resistance in predators and parasites of milkweed herbivores. *Curr. Biol.* **31**, R1465–R1466 (2021).

32. M. Lunzer, G. B. Golding, A. M. Dean, Pervasive cryptic epistasis in molecular evolution. *PLoS Genet* **6**, e1001162 (2010).

33. L. Yang, *et al.*, Predictability in the evolution of Orthopteran cardenolide insensitivity. *Philos. Trans. R. Soc. B* **374**, 20180246 (2019).

34. A. Stoltzfus, D. M. McCandlish, Mutational Biases Influence Parallel Adaptation. *Mol. Biol. Evol.* **34**, 2163–2172 (2017).

35. J. Zhang, S. Kumar, Detection of convergent and parallel evolution at the amino acid sequence level. *Mol. Biol. Evol.* **14**, 527–536 (1997).

36. L. F. Toledo, R. Ribeiro, C. F. Haddad, Anurans as prey: an exploratory analysis and size relationships between predators and their prey. *J. Zool.* **271**, 170–177 (2007).

37. S. Dobler, *et al.*, New ways to acquire resistance: imperfect convergence in insect adaptations to a potent plant toxin. *Proc. R. Soc. B* **286**, 20190883 (2019).

38. M. V. Clausen, F. Hilbers, H. Poulsen, The structure and function of the Na, K-ATPase isoforms in health and disease. *Front. Physiol.* **8**, 371 (2017).

39. J. A. Wells, Additivity of mutational effects in proteins. *Biochemistry* **29**, 8509–8517 (1990).

40. M. Lunzer, S. P. Miller, R. Felsheim, A. M. Dean, The biochemical architecture of an ancient adaptive landscape. *Science* **310**, 499–501 (2005).

41. L. I. Gong, M. A. Suchard, J. D. Bloom, Stability-mediated epistasis constrains the evolution of an influenza protein. *Elife* **2**, e00631 (2013).

42. P. Nosil, *et al.*, Ecology shapes epistasis in a genotype–phenotype–fitness map for stick insect colour. *Nat. Ecol. Evol.* **4**, 1673–1684 (2020).

43. B. J. Haas, *et al.*, De novo transcript sequence reconstruction from RNA-seq using the Trinity platform for reference generation and analysis. *Nat. Protoc.* **8**, 1494–1512 (2013).

44. D. Darriba, *et al.*, ModelTest-NG: a new and scalable tool for the selection of DNA and protein evolutionary models. *Mol. Biol. Evol.* **37**, 291–294 (2020).

45. A. Stamatakis, RAxML version 8: a tool for phylogenetic analysis and post-analysis of large phylogenies. *Bioinformatics* **30**, 1312–1313 (2014).

46. S. Guindon, *et al.*, New algorithms and methods to estimate maximum-likelihood phylogenies: assessing the performance of PhyML 3.0. *Syst. Biol.* **59**, 307–321 (2010).

678 47. G. Yu, D. K. Smith, H. Zhu, Y. Guan, T. T. Lam, ggtree: an R package for visualization and
679 annotation of phylogenetic trees with their covariates and other associated data. *Methods*
680 *Ecol. Evol.* **8**, 28–36 (2017).

681 48. Z. Yang, PAML 4: phylogenetic analysis by maximum likelihood. *Mol. Biol. Evol.* **24**, 1586–
682 1591 (2007).

683 49. G. Petschenka, *et al.*, Stepwise evolution of resistance to toxic cardenolides via genetic
684 substitutions in the Na+/K+-ATPase of milkweed butterflies (Lepidoptera: Danaini).
685 *Evolution* **67**, 2753–2761 (2013).

686 50. H. H. Taussky, E. Shorr, A microcolorimetric method for the determination of inorganic
687 phosphorus. *J. Biol. Chem.* **202**, 675–685 (1953).

688

689

Figures and Tables

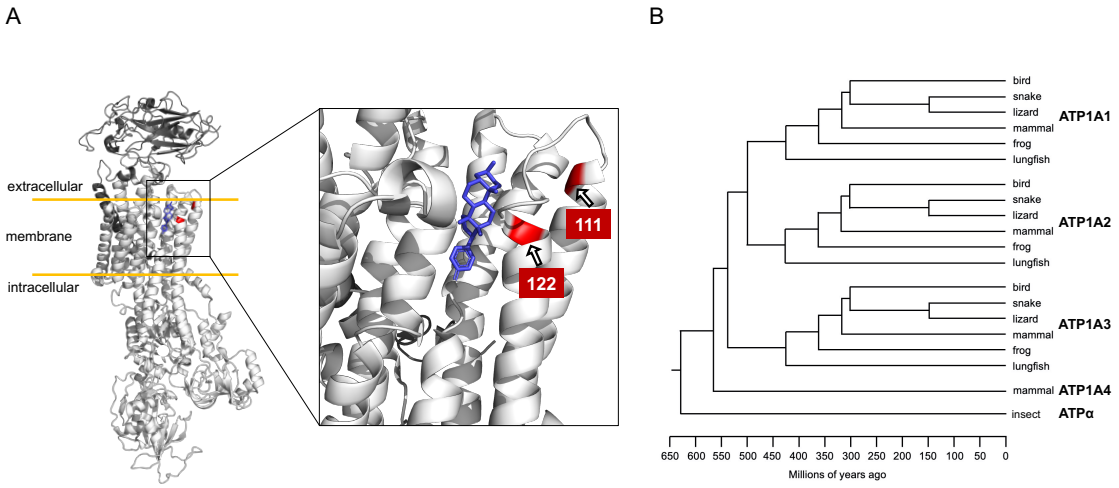

Figure 1. Na^+,K^+-ATPase structure and phylogenetic relationships of ATP1A paralogs among vertebrates. (A) Crystal structure of an Na^+,K^+-ATPase (NKA) with a bound the representative CTS bufalin in blue (PDB 4RES). The zoomed-in panel shows the H1-H2 extracellular loop, highlighting two amino acid positions (111 and 122 in red) that have been implicated repeatedly in CTS resistance. We highlight key examples of convergence in amino acid substitutions at sites in the H1-H2 extracellular loop associated with CTS resistance in Fig 3. (B) Phylogenetic relationships among ATP1A paralogs of vertebrates and ATPα of insects.

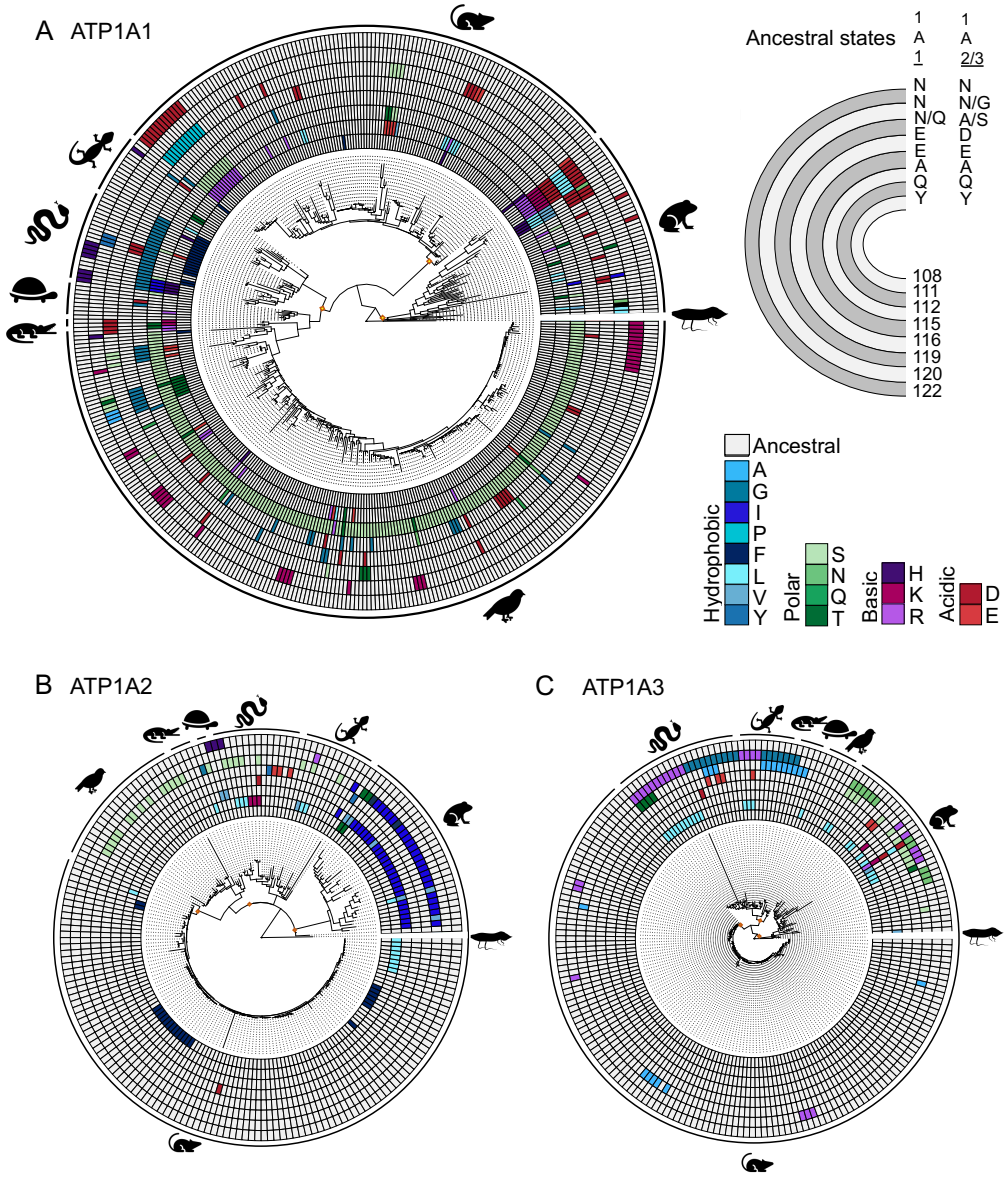

Figure 2. Patterns of molecular evolution in the α(M1–M2) extracellular loop of ATP1A paralogs shared among tetrapods. (A) Maximum likelihood phylogeny of tetrapod ATP1A1, (B) ATP1A2, and (C) ATP1A3. The character states for eight sites relevant to CTS resistance in and near the H1-H2 loop of the NKA protein are shown at the node tips. Yellow internal nodes indicate ancestral sequences reconstructed to infer derived amino acid states across clades to ease visualization; nodes reconstructed: MRCA of mammals, reptiles, and amphibians. *Top right*, each semi-circle indicates the site mapped in the main phylogeny with the inferred ancestral amino acid state for each of the three yellow nodes (posterior probability >0.8). In ATP1A1, site 119 was inferred as Q119 for amphibians and mammals, and N119 for reptiles (Table S6); in ATP1A2-3 site 119 was inferred as A119 for amphibians and reptiles, and S119 for mammals (Table S6). Site number corresponds to pig (*Sus scrofa*) reference sequence. Higher number and variation of substitutions in ATP1A1 stand out in comparison to the other paralogs.

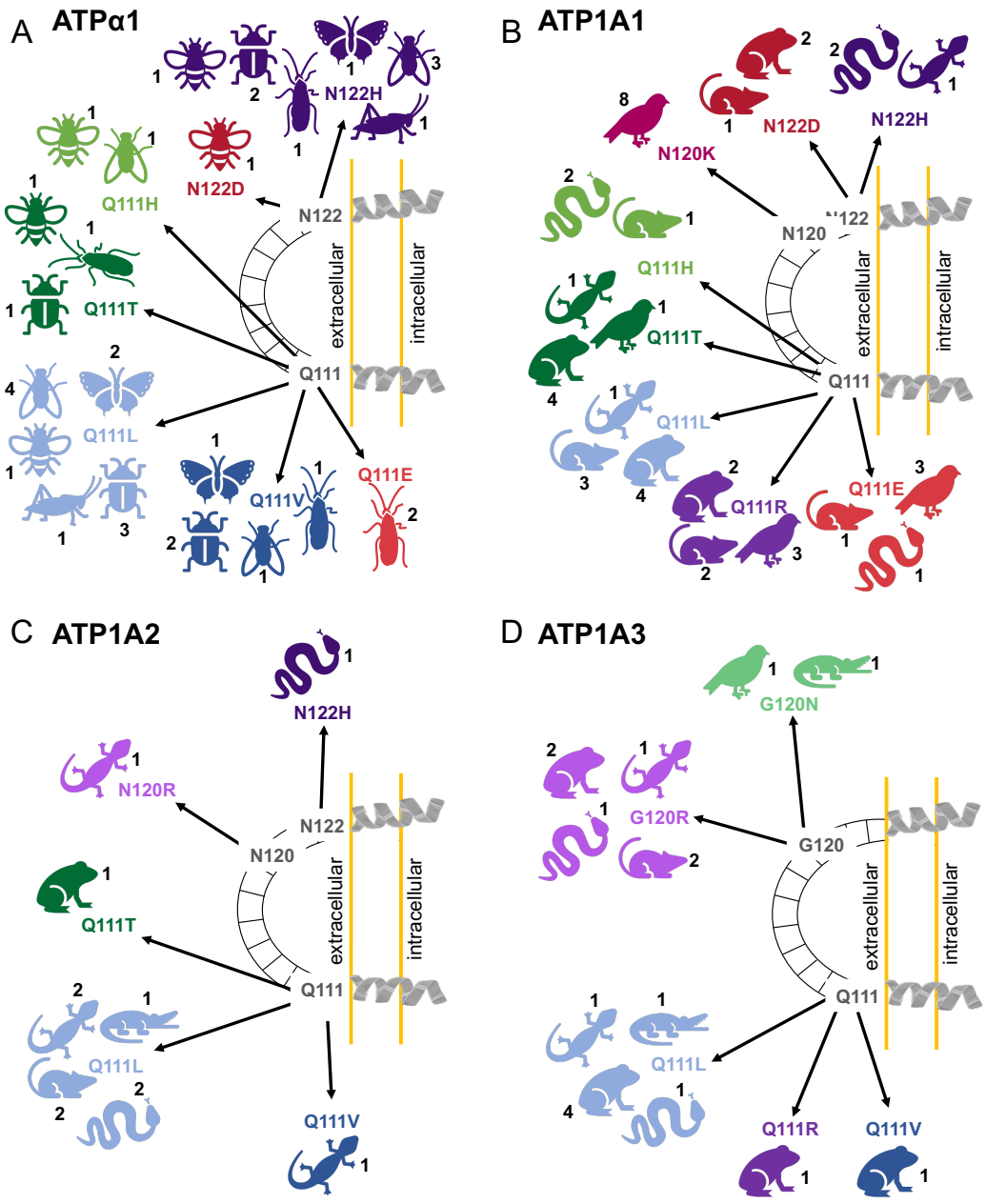

Figure 3. Parallel and divergent patterns of CTS-resistant substitutions across ATPα1 of insects and the shared ATP1A paralogs of tetrapods. Examples of convergence in ATPα1 across insects (A). Convergence in the **(B)** ATP1A1, **(C)** ATP1A2, and **(D)** ATP1A3 paralogs, respectively, across tetrapods. Numbers indicate the number of independent substitutions in each major clade depicted. For ATP1A3, resistance-conferring amino acid substitutions have been identified at site 120, and not 122. A full list of amino acid substitutions can be found in Supplementary Dataset 2 for tetrapods, and Taverner et al. (23) for insects.

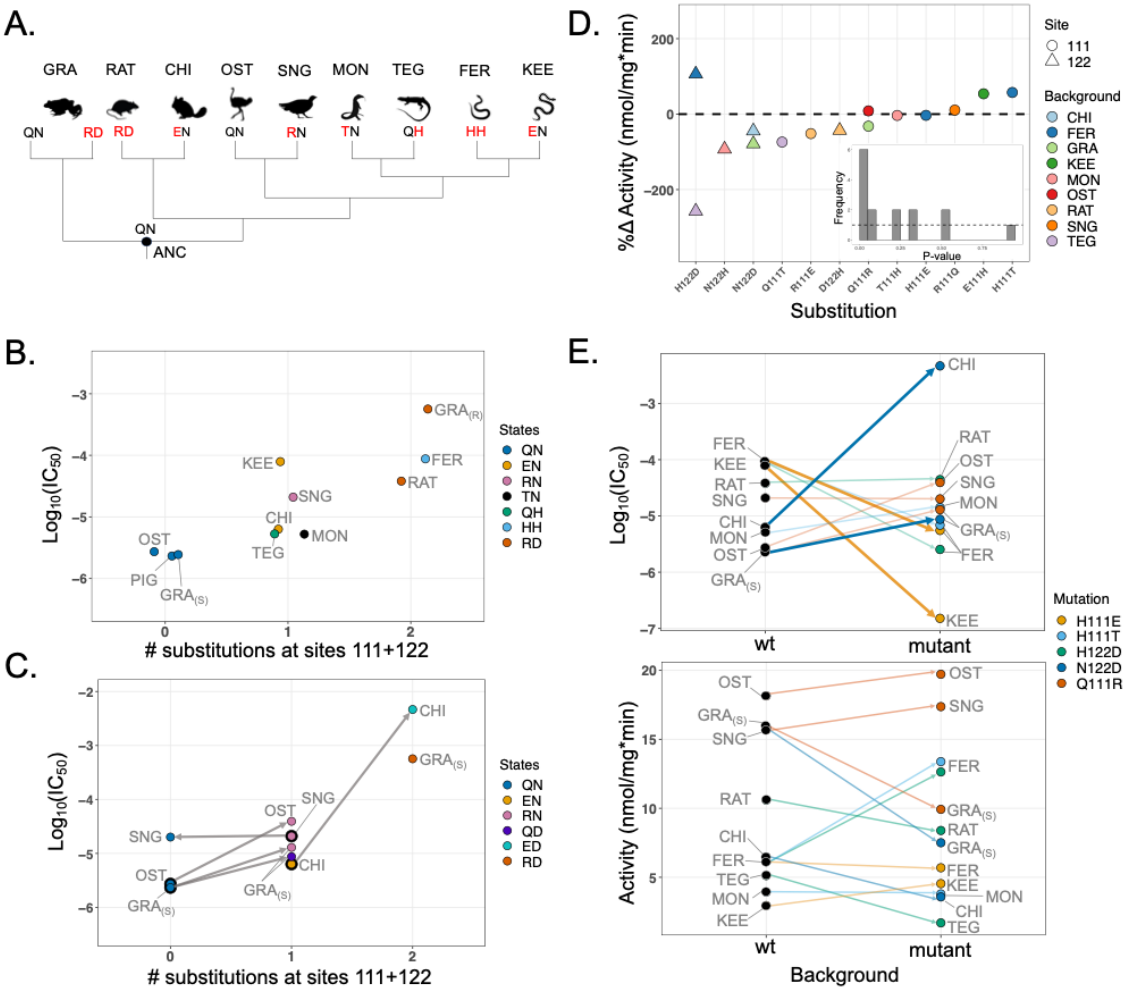

728

729 **Figure 4. Functional properties of wild-type and engineered ATP1A1**. **(A)** Cladogram
730 relating the surveyed species. GRA: Grass Frog (*Leptodactylus*); RAT: Rat (*Rattus*); CHI:
731 Chinchilla (*Chinchilla*); OST: Ostrich (*Struthio*); SNG: Sandgrouse (*Pterocles*); MON: Monitor
732 lizard (*Varanus*); TEG: Tegu lizard (*Tupinambis*); FER: False fer-de-lance (*Xenodon*); KEE: Red-
733 necked keelback snake (*Rhabdophis*). Two-letter codes underneath each avatar indicate native
734 amino acid states at sites 111 and 122, respectively. Data for grass frog from Mohammadi et al.
735 (2021). **(B)** Levels of CTS resistance (IC50) among wild-type enzymes. The x-axis distinguishes
736 among ATP1A1 with 0, 1 or 2 derived states at sites 111 and 122. The subscripts S and R refer
737 to the CTS-sensitive and CTS-resistant paralogs, respectively. **(C)** Effects of changing the
738 number of substitutions at 111 or 122 on CTS resistance (IC50). Substitutions result in
739 predictable changes to resistance except in the reversal R111Q in Sandgrouse (SNG). GRA_S
740 represents Q111R+N122D on the sensitive paralog background. **(D)** Effects of single
741 substitutions on Na^+,K^+-ATPase (NKA) activity. Each modified ATP1A1 is compared to the wild-
742 type enzyme for that species. The inset shows the distribution of *t*-test p-values for all 15
743 substitutions, with the dotted line indicating the expectation**. (E)** Evidence for epistasis for CTS
744 resistance (IC50, upper panel) and lack of such effects for enzyme activity (lower panel). Each
745 line compares the same substitution (or the reverse substitution) tested on at least two
746 backgrounds. Thicker lines correspond to substitutions with significant sequence-context
747 dependent effects (Bonferroni-corrected ANOVA p-values < 0.05, Table S5).

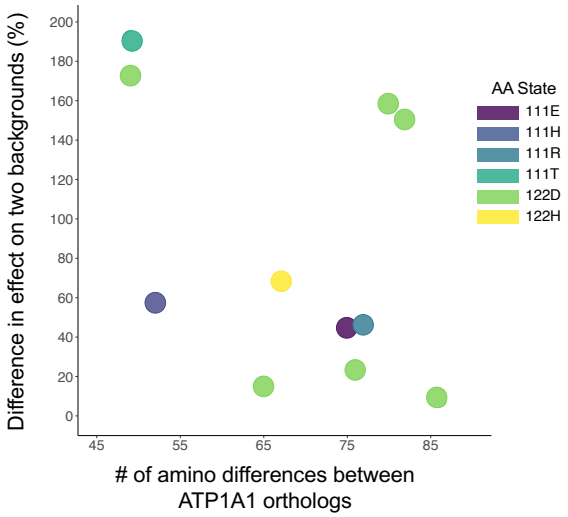

Figure 5. No relationship between the effect of substitution to a given amino state on activity and the extent of divergence between ATP1A1 orthologs. Each point represents a comparison between the effect (% change in activity relative to the wild-type enzyme) of a given amino acid state (e.g., 122D) on two different genetic backgrounds. For example, the effect of 122D between chinchilla and false fer-de-lance is measured as % change [chinchilla vs. chinchilla+N122D] minus the % change [false fer-de-lance vs. false fer-de-lance+H122D]. Comparisons were measured as the difference between the two effects. In total, 11 comparisons were possible. The x-axis represents the number of amino acid differences between two ATP1A1 proteins being compared. Assuming intramolecular epistasis for protein function is prevalent, a positive correlation is predicted. However, no such relationship is observed (Spearman's correlation, r_S = -0.42, p = 0.19).

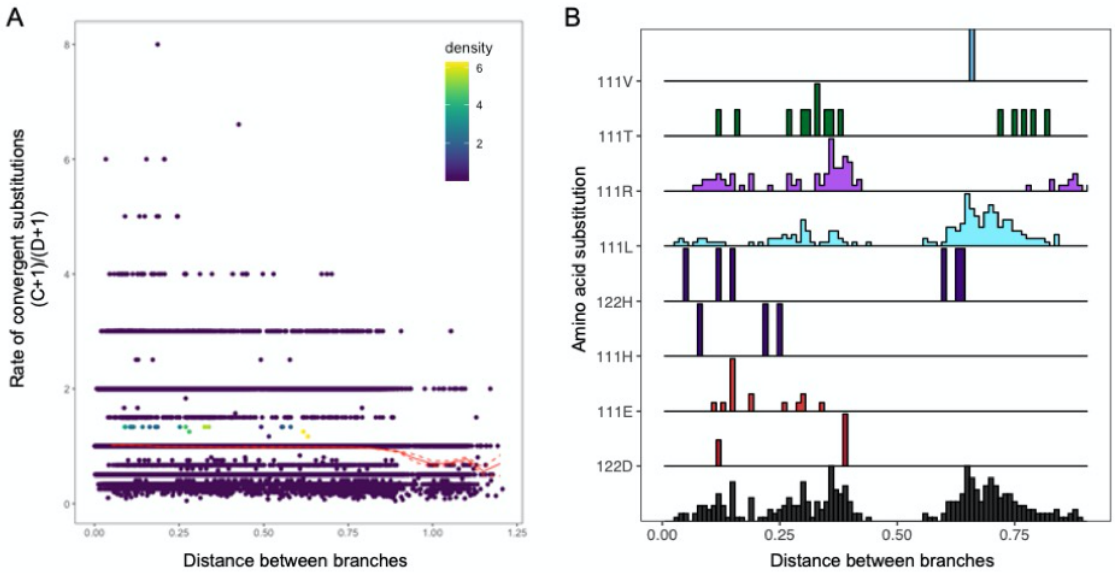

Figure 6. Rate of convergence across ATP1A sequences as a function of increasing sequence divergence. (A) Change in the rate of convergence (protein wide) over time for the ATP1A protein family. The proportion of convergent (C) over divergent (D) substitutions along the entire protein sequence was estimated for all pairs of branches in the ATP1A phylogeny, except for sister branches or ancestor-descendant pairs. Color scale shows the density of dots for both axes. The distance between branches corresponds to the expected number of amino acid substitutions per site between protein pairs being compared (under the JTT+G4+F model). The red line shows a running average with a window size of 0.05 substitutions/site. Dashed lines show the 95% confidence interval based on 100 bootstrap replicates per window. **(B)** For each derived amino acid state at sites 111 and 122, the histograms show the distribution of pairwise convergent events along the sequence divergence axis (expected number of substitutions per site). Substitutions are color coded as in Figure 2. The histogram at the bottom shows the combined distribution of pairwise convergent events for both sites.